Neurochemical Research (2025) 50:160
https://doi.org/10.1007/s11064-025-04411-0

RESEARCH

Effects and Mechanisms of Paeoniflorin in Relieving Neuropathic Pain: Network Pharmacological Analysis and Experimental Validation

Fangning Xu[1] · Qingzhen Liu[2] · Shenquan Cai[2] · Qiuyan Yu[2] · Yue Zhang[3] · Zhi Liu[2] · Haishu Zhao[2] · Lidong Zhang[1]

Received: 17 September 2024 / Revised: 27 February 2025 / Accepted: 28 April 2025

Abstract

Neuropathic pain (NP) is a prevalent condition that can lead to a variety of complications, significantly impacting patients' quality of life. Previous studies have confirmed that paeoniflorin (PF) demonstrates both therapeutic pain relief and neuroprotective effects. However, its therapeutic efficacy in managing NP remains to be thoroughly investigated. We conducted a systematic study to explore the underlying mechanisms of PF in the treatment of NP through combining network pharmacological analysis with experimental validation. Our studies revealed that PF alleviates NP through a multifaceted approach, mainly involving protein kinase C (PKC), serotonin receptors, calcium signaling pathways, inflammatory mediator regulation of transient receptor potential (TRP) channels, and G-protein coupled receptor signaling pathways. Additionally, our animal experiments indicated that PF reduces pain-related behavior on spinal nerve ligation-induced NP in rats by modulating the PKCε-TRPV1 pathway. PF was found to inhibit the expression of inflammatory factors such as interleukin 6 and tumor necrosis factor α, as well as the activation of microglia, thereby alleviating NP. These findings suggest a potential therapeutic role for PF in the treatment of NP, providing a valuable reference for clinical applications.

Keywords Neuropathic pain · Paeoniflorin · Microglia · Network pharmacology · TRPV1 · PKC

Introduction

Neuropathic pain (NP) is characterized by a series of unpleasant sensations triggered or caused by primary damage and dysfunction of the nervous system, and it is classified as a type of chronic pain. The prevalence of NP can reach up to 10% of the global population. Furthermore, 60% of patients with NP also suffer from complications such as depression, anxiety, and sleep disorders, which significantly impair their quality of life [1]. There is a strong clinical association between NP and mood changes as well as stress disorders; however, the exact physiological mechanisms underlying this relationship remain unclear [2]. Due to the complexity and diversity of NP pathogenesis, the main studies have focused on several key factors, including abnormal ectopic activity of injured nerves, peripheral and central sensitization, impaired inhibitory regulation, and pathological activation of microglia [3]. Clinically, the treatment of NP primarily relies on pharmacologic therapy. First-line drugs include tricyclic antidepressants, gabapentin, pregabalin, and serotonin-norepinephrine reuptake inhibitors. Despite evidence supporting their efficacy through different mechanisms, the effect sizes are generally small, many patients do not achieve adequate pain relief at tolerated doses, and often accompanied by side effects [4]. Consequently, it is imperative to explore more effective therapeutic agents or strategies with fewer side effects to alleviate NP.

Traditional Chinese medicine (TCM) is renowned for its multi-directional, multi-target, and multi-pathway approaches in disease treatment, often resulting in fewer side effects. A key component of TCM formulas, White Paeony Root, is known for its diverse therapeutic properties,

✉ Qingzhen Liu
liuqingzhen198211@163.com

✉ Lidong Zhang
ldzhang1968@163.com

[1] Department of Anesthesiology, Jinling Clinical Medical College, Nanjing University of Chinese Medicine, Nanjing, Jiangsu Province 210008, P. R. China

[2] Department of Anesthesiology, Jinling Hospital, Affiliated Hospital of Medical School, Nanjing University, Nanjing, Jiangsu Province 210008, P. R. China

[3] Department of Anesthesiology, Jinling Hospital, Medical College of Nanjing Medical University, Nanjing, Jiangsu Province 210008, P. R. China

Published online: 09 May 2025

including hemostasis, menstrual regulation, yin astringency, sweat inhibition, pain alleviation, and calming of liver yang [5]. The Shen Nong Ben Cao Jing, also known as The Divine Husbandman's Classic of the Materia Medica, documents the medicinal properties of Paeony, highlighting its use in dispelling evil Qi, alleviating abdominal pain, eliminating blood stasis, and treating chills, fever, and hernias. Additionally, it is noted for its ability to assuage pain, and facilitate urination, laying the foundation for its clinical application. The primary active ingredient in Paeony, particularly for treating pain, inflammation, and immune system disorders, is the total glucosides of paeony extracted from the dried White Paeony Root. Paeoniflorin (PF) is the main active component of these glucosides. PF has effectively treated inflammatory responses in animal models of autoimmune diseases, such as experimental arthritis, psoriasis in mice, and experimental autoimmune encephalomyelitis [6]. Numerous studies also have demonstrated PF's cardiovascular and neuroprotective effects, as well as its anti-inflammatory, antidepressant, and immunomodulatory properties [6, 7]. Recent researches have shown that PF reduces pain in animal models of inflammation, postoperative conditions, and dysmenorrhea [8–10]. In addition, recent studies have shown that PF plays a role in alleviating pain behaviors in various NP models. Zhou Danli et al. demonstrated that PF can inhibit neuroinflammation in rats with Chronic Constrictive Injury by reducing the phosphorylation of ASK1, p-p38, and p-JNK, thereby delaying the progression of NP [11]. Tsugunobu Andoh et al. reported that PF activates the adenosine A1 receptor, protecting sensory nerves from demyelination and effectively alleviating paclitaxel-induced mechanical allodynia, suggesting that PF may be beneficial for pain relief associated with NP [12]. Furthermore, the combined application of PF and Liquiritin can alleviate NP in the Spared Nerve Injury (SNI) model by restoring the mechanical withdrawal threshold and modulating the expression of Glial Fibrillary Acidic Protein and Ionized Calcium-Binding Adapter Molecule 1 (IBA1) [13]. Nevertheless, the exact mechanisms by which PF alleviates NP remain incompletely understood. Its effects may involve multiple signaling pathways and cellular mechanisms, including the inhibition of neuroinflammation, modulation of glial cells, and improvement of neuronal survival. Therefore, a deeper elucidation of the underlying mechanisms of PF, along with the exploration of its clinical applications in treating NP, holds significant scientific and clinical importance.

Network pharmacology, a new discipline grounded in systems biology theory, biological systems network analysis, and multi-target drug molecular design, is characterized by its integrity, systematization, and comprehensiveness [14]. The application of network pharmacology can significantly aid in elucidating the exact mechanisms underlying the therapeutic effects of Chinese medicines on various diseases. In this study, we aim to comprehensively investigate the protective effects and action mechanisms of PF on NP utilizing network pharmacological analysis methods and animal experimental studies, to provide a reference basis for the clinical use of PF in the treatment of NP (Fig. 1).

Methods

PF and NP Common Target Acquisition

The protein targets of PF were initially predicted using the TCMSP (https://old.tcmsp-e.com/tcmsp.php) and Swiss Target Prediction (http://www.swisstargetprediction.ch/) databases. Subsequently, the names of these protein targets were standardized through the UniProt database (https://www.uniprot.org/). To obtain target information related to NP, the GeneCards(https://www.genecards.org/), OMIM (https://www.omim.org/), and DrugBank (https://go.drugbank.com/) databases were queried using the keyword "Neuropathic pain." Venny 2.1 was employed to identify overlapping targets between PF and NP, and a Venn diagram was generated to visualize these intersections.

Protein Interaction Network Construction and Analysis

Protein–protein interaction (PPI) between PF and NP targeted proteins was analyzed using the STRING database (https://string-db.org/), which contains extensive information on PPI. The resulting protein interaction data were imported into Cytoscape 3.10.0 software to visualize the PPI network and calculated the degree of each protein node. In the PPI network, nodes symbolize protein targets, and connections between nodes indicate interactions between these proteins. The degree of a node, which signifies the number of connections it possesses, serves as an indicator of the protein's significance within the network. Therefore, we can identify key protein targets based on degree.

Biological Function and Pathway Analysis of Genes

Gene Ontology (GO) enrichment analysis and Kyoto Encyclopedia of Genes and Genomes (KEGG) pathway analysis were conducted using the DAVID database (https://david.ncifcrf.gov/). The therapeutic targets for PF to alleviate NP were submitted to the DAVID database for further analysis. GO enrichment analysis was performed across three categories: biological processes (BP), cellular components (CC), and molecular functions (MF). The top 10 GO enriched terms, with a $p\text{-}value < 0.01$ and false discovery rate

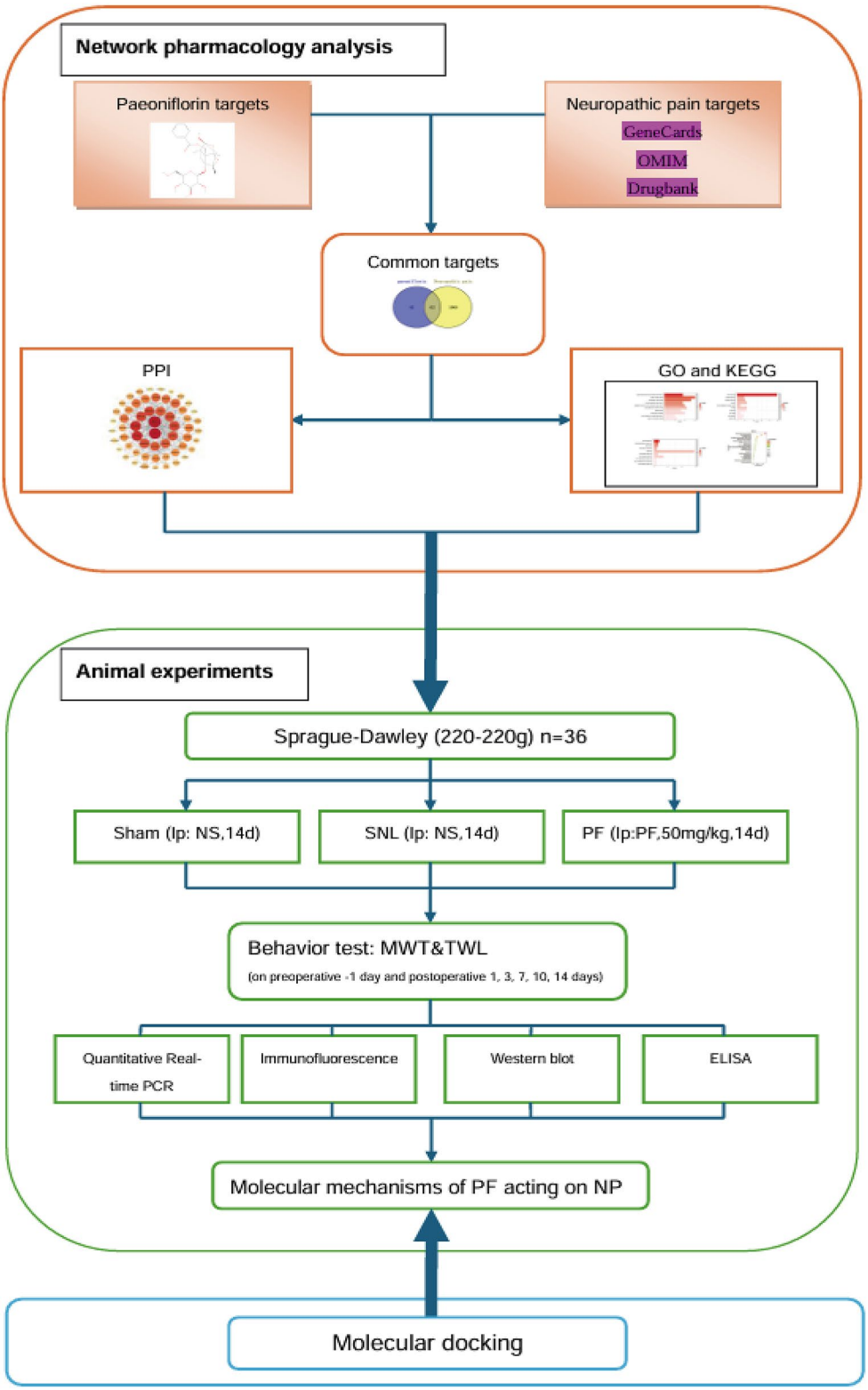

Fig. 1 Schematic diagram of the study of the molecular mechanism of pain by paeoniflorin to relieve neuropathic pain

(FDR) < 0.05 were selected for detailed analysis [15]. Similarly, the top 20 KEGG enriched terms, meeting the same statistical criteria, were chosen for further investigation. Finally, the Bioinformatics platform (http://www.bioinformatics.com.cn/) was used to generate bar graphs for GO enrichment analysis and bubble graphs for KEGG pathway analysis.

Animals

A total of 36 adult male Sprague-Dawley (SD) rats (SPF, 6–8 weeks old, 200–220 g) were obtained from Henan Skobes Biotechnology Co., Ltd (China) [Production License No: SCXK(Yu)2020-0005]. All rats had free access to food and water, were kept at a room temperature of 20 to 25 °C, with a humidity of 25–30%, and were maintained under a 12-hour light-dark cycle. This experiment was approved by the Experimental Animal Use and Management Committee of the General Hospital of Eastern Theater Command (Approval No. DZYGKTZY240004), which conformed to the requirements related to experimental animal welfare and ethics.

Animal Model Preparation

The spinal nerve ligation (SNL) rat model was established following the method described by Kim [16]. Rats were anesthetized with pentobarbital sodium (40 mg/kg, intraperitoneal) and positioned prone on a surgical platform. A longitudinal incision was made at the lower lumbar and sacral levels, followed by blunt separation of the fascia and muscle. The right L6 transverse process was slightly removed to expose the L4 and L5 spinal nerves. Subsequently, the L5 spinal nerve was ligated using a 4−0 suture, and hemostasis was achieved with a cotton swab. The muscles and skin were then sutured in layers using silk thread. In the sham surgery group, the right L5 spinal nerve was exposed but not ligated.

Experimental Grouping

After a one-week acclimatization and feeding period, 36 SD rats were randomly assigned to three groups ($n=12$): the sham surgery group (Sham group), the SNL model group (SNL group), and the SNL model + PF group (PF group). The PF group received intraperitoneal injections of 50 mg/kg PF (analytical purity of 98%, Macklin Biochemical Technology, P815485, Shanghai, China) once daily for 14 days, beginning on the first day after SNL surgery [17]. In contrast, the Sham and SNL groups were administered an equivalent volume of normal saline. Behavioral assessments were conducted one day before SNL surgery (day 0, baseline) and on days 3, 7, 10, and 14 post-SNL surgery, with measurements taken one hour after treatment administration. On the 14th day following SNL surgery, spinal cord tissue from the rats was collected for further analysis after the behavioral studies (Fig. 3a).

Behavioral Tests

Mechanical Withdrawal Threshold (MWT)

The rats were placed in a plexiglass box with metal mesh at the bottom and allowed to acclimate to the environment for 30 min. Next, Von Frey fiber filaments of varying strengths (2, 4, 6, 8, 10, 15, and 26 g) were applied vertically to the middle of the right hind paw of each rat. The stimulus strength was determined by the bending of the filaments, which were held in place for 5 s. The up-down method and the specific formula ($50\%MWT(g)=10^{[Xf+k\delta]}/10000$;[Xf] is the number of the last test Von Frey fiber filaments, [δ] is the mean difference after the logarithms of the gram number of each fiber filament, and [k] is the coefficient obtained by measurement.) was used to get the final mechanical pain contraction foot threshold [18].

Thermal Withdrawal Latency (TWL)

For the TWL assessment, rats were placed in plexiglass compartments with a glass platform at the bottom and allowed to adapt to the environment for 30 min. A thermal radiation stimulator was positioned beneath the glass platform, with the light source focused vertically on the surface of the right hind paw of each rat. The latency time was recorded until the rats either licked or raised their foot, with an automatic cut-off time set at 30 s. This process was repeated five times with a 5-minute interval between each trial. The results of the five measurements were averaged, excluding the maximum and minimum values, and the average value was recorded as the TWL (s).

Quantitative Real-Time Polymerase Chain Reaction (qPCR)

Following the induction of deep anesthesia with pentobarbital sodium (50 mg/kg, intraperitoneal), the hearts of the rats were injected with pre-cooled phosphate-buffered saline (PBS) solution. The L4-L6 segments of the spinal cord were dissected on ice and rapidly frozen using liquid nitrogen. The frozen tissues were then placed into pre-cooled grinding tubes containing RNA extraction solution (Servicebio, China) and grinding beads to facilitate the extraction of total RNA. The RNA concentration and purity were assessed using a Nanodrop 2000 spectrophotometer. RNA samples with excessive concentration were diluted to achieve a final concentration of 200ng/μl. The reverse transcription reaction system (Servicebio, China) was prepared, gently mixed, and centrifuged. The reverse transcription program was executed with the following thermal cycling conditions: 25 °C for 5 min, 42 °C for 30 min, and 85 °C for 5 s. All primers used for PCR amplification were procured from Wuhan Servicebio

Technology Co., Ltd., with the primer sequences detailed in Table 1. The PCR reaction mixture was sealed and centrifuged in a microplate centrifuge before being subjected to fluorescence quantitative PCR. The PCR amplification protocol included an initial denaturation at 95 ℃ for 30 s, followed by 40 cycles of 95 °C for 15 s and annealing at 60 °C for 30 s. Relative gene expression levels were quantified using the $2^{-\Delta\Delta CT}$ method.

Immunofluorescence

Deeply anesthetized rats were transcardially perfused with PBS followed by 4% paraformaldehyde. The L4 to L6 segments of the spinal cords were then collected and fixed in the same 4% paraformaldehyde for 24 h. Following fixation, the tissue specimens underwent dehydration in a 30% sucrose solution, embedded in paraffin, and sectioned at 4 μm thickness. The sections were subsequently blocked in a 3% bovine serum albumin-blocking solution for 30 min. After washing with PBS, the primary antibody IBA1(Rabbit pAb, lgG, 1:500, Servicebio, China) was added and incubated overnight at 4 °C. The sections were washed again and incubated with the secondary antibody at room temperature for 50 min, protected from light. Following another PBS wash, DAPI staining solution was added to reverse stain the nucleus, and the sections were incubated for 10 min at room temperature, away from sunlight. The slides were then incubated in PBS for an additional 10 min. Finally, images were captured, and cell count quantification was performed using ImageJ software.

Western Blotting

Under anesthesia, rats were perfused through the heart with pre-cooled PBS solution. The L4-L6 spinal cord tissue was then dissected out on ice and snap-frozen in liquid nitrogen. Subsequently, the spinal cord tissues were homogenized on ice in RIPA lysis buffer containing 1% proteinase and phosphatase inhibitors (Beyotime, China). The total protein concentration was determined using a BCA protein assay kit (Epizyme, China). The total protein samples were diluted to a concentration of 2 mg/ml with pre-cooled PBS and SDS-PAGE Sample Loading Buffer. Proteins were separated by SDS-PAGE gel electrophoresis and transferred to a PVDF membrane. The membrane was then treated with a rapid closure solution (Servicebio, China) for 15 min at room temperature. Following this, the membrane was washed three times with 0.1% Tris -buffered saline with Tween (TBST), and incubated and incubated overnight at 4 °C with primary antibodies against β-actin (Rabbit mAb, lgG, 1:50000, ABclonal, China), transient receptor potential vanilloid 1(TRPV1, Rabbit pAb, lgG,1:1000, ABclonal, China), protein kinase C ε (PKCε, Rabbit pAb, lgG 1:1000, ABclonal, China), IBA1 (1:5000, Rabbit pAb, lgG, Gene Tex, USA). All antibodies were prepared with TBST solution. After three additional washes with TBST, the membrane was incubated for 1 h at room temperature with secondary antibodies (HRP-conjugated Goat Anti-Rabbit IgG(H+L),1:5000, Proteintech, China) conjugated to horseradish peroxidase. Finally, the immunofluorescence bands were visualized using a chemiluminescence and epifluorescence imaging system (Alliance Q9 Advanced, Uvitec, UK), and analyzed using ImageJ software.

Enzyme Linked Immunosorbent Assay (ELISA)

After the deep anesthesia of the rats, their hearts were perfused with pre-cooled PBS solution. The L4-L6 segments of the spinal cord were dissected and rapidly frozen in liquid nitrogen. The spinal cord tissues were then homogenized in pre-cooled PBS containing 1% protease and phosphatase inhibitors using an ultrasonic crusher. The total protein content was normalized utilizing a BCA protein assay kit. Protein levels of interleukin 6 (IL-6) and tumor necrosis factor α (TNF-α) were quantified using ELISA kits specific for IL-6 and TNF-α (Lianke, China), following the instructions provided by the manufacturer.

Table 1 Specific primer sequences

Primer information	Gene name	Upstream primer sequence(5'-3')	Downstream primer sequence(5'-3')	Fragment length(bp)
NM_031982.1	TRPV1	CCTATCATCACTGTCAGCTC TGTTC	TCTGGGTCTTTGAAC TCGCTGT	236
NM_017171.2	PKCε	GAAGAACGAGTGTTTAGGG AGCG	CGACGCAGGTACAA ACTTGACAT	196
NM_012589.2	IL-6	GAGTTGTGCAATGGCAATT CTG	ACGGAACTCCAGAA GACCAGAG	162
NM_012675.3	TNF-α	TACTGAACTTCGGGGTGAT CG	AGAAGATGATCTGA GTGTGAGGGTC	104
XM_006256063.3	IBA1	GCTCCGAGGAGACGTTCAG TTAC	GTTGGCTTCTGGTGT TCTTTGTTT	118
NM_017008.4	GAPDH	CTGGAGAAACCTGCCAAGT ATG	GGTGGAAGAATGGG AGTTGCT	138

Molecular Docking

The three-dimensional (3D) structure of and protein targets were retrieved from the RCSB Protein Data Bank database (https://www.rcsb.org/), and the PDB ID information is listed in Table 3. Chemical 3D structure of PF, the PKCε inhibitor Sotrastaurin (AEB071), and the TRPV1 selective antagonist SB-366,791 were retrieved from PubChem database (https://pubchem.ncbi.nlm.nih.gov/). Those compound s as the ligands were blind docked with target proteins by the online CB-Dock2 database (https://cadd.labshare.cn/cb-dock2/php/index.php) for validation and visualization analysis. CB-Dock2 employs a curvature-based cavity detection method to predict the binding region of a given protein and determine the center and size of this region [19]. Generally, results of molecular docking are primarily assessed by minimum binding energies. Lower binding energies suggest that less energy is needed for the drug molecule to bind with the target, indicating greater binding potential and stability [20].

Statistical Processing Results

Data analysis was conducted using GraphPad Prism 9.0 software, with results presented as mean ± SD. The Shapiro-Wilk test and Brown-Forsythe test were employed to assess normal distribution and homoscedasticity. When both conditions were satisfied, a one-way ANOVA followed by Tukey's post-hoc test was applied for comparisons among multiple groups. In cases where normal distribution and homoscedasticity were not met, the Kruskal-Wallis test was used as an alternative. For repeated measurement data across multiple groups, a two-way ANOVA with Tukey's post-hoc test was utilized. Additionally, curve estimation and linear regression analyses were conducted to explore correlations. Differences were considered to be statistically significant when the $P<0.05$.

Results

Identification of Potential Therapeutic Targets for PF against NP

Multiple database searches and predictions yielded 104 action targets for PF protein and 2,022 targets for NP. By intersecting these PF drug targets with NP targets, we identified 62 potential therapeutic targets for PF against NP (Fig. 2a).

Interaction Network Analysis of Potential Therapeutic Targets

These 62 targets were then input into the String database to construct a PPI network, which was subsequently visualized using Cytoscape 3.6.10 software (Fig. 2b). Analysis of the degree within this network predicted IL-6 and TNF as key targets for PF in the treatment of NP. The degree of each target in the PPI network is shown in Table 2. We performed molecular docking analysis on proteins with a degree value greater than 15, and the results are detailed in Table 3; Fig. 5a and o. The analytical data reveal that the binding energies of all docked complexes are below 7.5 kcal/mol, suggesting that PF can form stable interactions with these proteins. The calculated binding energies further confirm the high affinity between PF and the target proteins.

GO Enrichment Analysis and KEGG Signaling Pathway Analysis

Further investigation through KEGG signaling pathway and GO enrichment analysis of the 62 potential therapeutic targets revealed that PF is involved in several BP, including the adenylate cyclase-activating adrenergic receptor signaling pathway, response to xenobiotic stimulus, and positive regulation of the mitogen-activated protein kinase (MAPK) cascade (Fig. 2c). The CC affected by PF primarily include the plasma membrane, presynaptic membrane, and postsynaptic membrane (Fig. 2d). Additionally, PF is associated with various MF, such as PKC activity, G-protein coupled receptor (GPCR) activity, and serotonin (5-HT) binding (Fig. 2e). KEGG pathway analysis further indicated that PF is highly correlated with pathways involved in neuroactive ligand-receptor interactions, the calcium (Ca^{2+}) signaling pathway, serotonergic synapse, and the regulation of transient receptor potential (TRP) channels by inflammatory mediators (Fig. 2f). These findings suggest that PF alleviates NP through a multifaceted approach, targeting various BP, CC, and MF related to pain perception, signal transduction, and inflammatory pathways. Based on these results and supporting literature, we chose the PKC-TRPV1 pathway for experimental verification.

Characterizations of the SNL Model

The MWT and TWL were measured one day before surgery and at 3, 7, 10, and 14days post-surgery. As illustrated in Fig. 3b and c, SNL-induced rapid and persistent mechanical and heat hyperalgesia in the SNL group. Specifically, the rats in the SNL group exhibited significantly decreased MWT and TWL from day 3 to day 14 post-surgery compared to the Sham group (all $P<0.05$). Additionally, we assessed

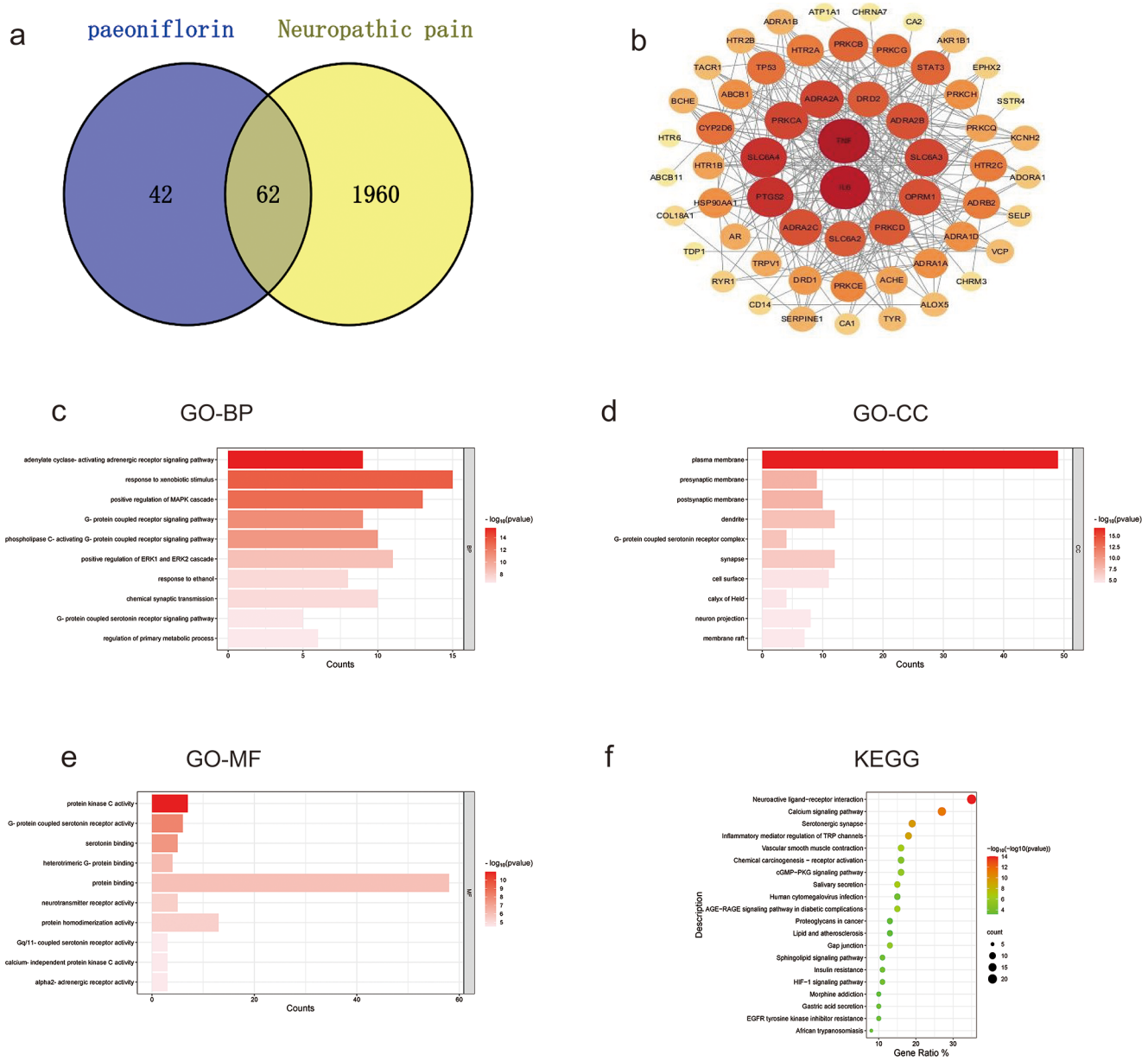

Fig. 2 Results of network pharmacologic analysis of paeoniflorin relieving NP. (**a**) The Venn diagram of common targets of paeoniflorin with NP. (**b**) PPI network of 62 common targets of paeoniflorin with NP. In the network graph, each node represents a different protein target and the node size represents the degree. The color of the nodes reflects the degree of connectivity (redder color indicates higher degree of connectivity). Straight lines represent protein relationships between targets. (**c**) GO enrichment analysis of common targets with NP-log10 (*p-value*) top 10 BP results. (**d**) Top10 CC results of GO enrichment analysis-log10 (*p-value*) for common targets. (**e**) Top 10 MF results of GO enrichment analysis-log10 (*p-value*) for common targets of paeoniflorin versus NP. (**f**) KEGG pathway analysis results for the top 20 of common targets-log10 (*p-value*) of paeoniflorin with NP

the expression levels of microglia marker IBA1 and inflammatory cytokines IL-6 and TNF-α in the spinal cord dorsal horn at 14 days post-SNL. The data, presented in Figs. 3f and h and 4e and h, revealed significantly higher mRNA and protein expression levels of IBA1, IL-6, and TNF-α in the SNL group compared to the Sham group (all $P<0.05$). These findings indicate that SNL induces microglia activation in the spinal cord.

PF Attenuated SNL-induced Mechanical Hyperalgesia and Heat Hyperalgesia in NP

Following the SNL surgery, the rats were randomly divided into the SNL group and the PF group. As depicted in Fig. 3b, PF attenuated mechanical hypersensitivity associated with SNL model. The results of MWT in SNL and PF groups indicated that PF began to exhibit antinociceptive

Table 2 The weighted degree of each target

Name	Degree	Name	Degree	Name	Degree	Name	Degree
TNF	24	PRKCG	14	ACHE	9	EPHX2	4
IL6	23	CYP2D6	14	TRPV1	8	RYR1	4
PTGS2	20	TP53	14	AR	8	CA1	4
SLC6A4	20	HTR2C	13	HTR2B	7	COL18A1	3
ADRA2A	18	HTR2A	13	SERPINE1	7	CD14	3
SLC6A3	18	ADRB2	13	BCHE	7	CHRM3	2
PRKCA	18	PRKCE	12	ADRA1B	7	TDP1	1
ADRA2C	17	PRKCH	11	KCNH2	7	SSTR4	1
ADRA2B	17	ADRA1D	11	VCP	6	HTR6	1
OPRM1	17	ADRA1A	11	ALOX5	6	CA2	1
PRKCD	16	HSP90AA1	11	AKR1B1	6	ATP1A1	1
SLC6A2	16	ABCB1	11	TACR1	6	CHRNA7	1
DRD2	16	DRD1	10	TYR	6	ABCB11	1
PRKCB	15	PRKCQ	9	ADORA1	5		
STAT3	15	HTR1B	9	SELP	4		

Table 3 The result of molecular Docking

Protein	PDB ID	Ligand	Binding energies (kcal/mol)	Center (x, y, z)	Docking size (x, y, z)
TNF-a	7DOV	paeoniflorin	-9	23, 19, -5	22, 22, 22
IL-6	8QY5	paeoniflorin	-8	285, 245, 259	22, 22, 22
PTGS2	3HS5	paeoniflorin	-10.4	25, 28, 43	35, 35, 35
SLC6A4	5I6Z	paeoniflorin	-10.1	46, 182, 153	35, 35, 35
ADRA2A	1HLL	paeoniflorin	-8.5	-5, -12, 10	22, 22, 22
SLC6A3	9EUP	paeoniflorin	-8.6	160, 165, 133	22, 22, 30
PRKCA	3HPM	paeoniflorin	-9.2	0, 2, 3	22, 22, 22
ADRA2C	6KUW	paeoniflorin	-10.3	-30, -11, 56	22, 22, 22
ADRA2B	6K41	paeoniflorin	-10.6	118, 110, 82	22, 35, 22
OPRM1	4DKL	paeoniflorin	-9	-27, -10, -10	22, 22, 22
PRKCD	3UEJ	paeoniflorin	-8.3	10, -3, 12	22, 22, 22
SLC6A2	8HFE	paeoniflorin	-10	113, 111, 115	22, 22, 28
DRD2	8TZQ	paeoniflorin	-10	165, 167, 190	22, 22, 22
PRKCB	3PFQ	paeoniflorin	-10.6	-43, 13, -17	28, 22, 22
STAT3	4ZIA	paeoniflorin	-7.7	130, 51, 125	22, 22, 22
PRKCE	2WHO	paeoniflorin	-8	55, 2, 41	22, 22, 22
PRKCE	2WHO	AEB071	-8.9	55, 2, 41	22, 22, 22
TRPV1	8GF8	paeoniflorin	-8.1	75, 100, 100	31, 30, 35
TRPV1	8GF8	SB-366,791	-8.2	75, 100, 100	31, 30, 35

effects after 7 consecutive days of intraperitoneal injection ($P<0.05$). It significantly improved MWT after 14 consecutive days of administration ($P<0.0001$) (Fig. 3b). Additionally, as illustrated in Fig. 3c, TWL measurements revealed that administering PF for 10 consecutive days increased TWL, and a significant reduction in SNL-induced hyperalgesia symptoms was observed after 14 consecutive days of administration ($P<0.001$). Besides, no statistical significance was observed in MWT and TWL between PF and Sham groups after 7 consecutive days of administration.

PF Alleviated NP Through PKCε-TRPV1 Signaling Pathway

Based on the results of network pharmacology GO and KEGG enrichment analysis, the PKCε-TRPV1 pathway in the TRP channel regulated by inflammatory mediators was selected for verification. The Western blotting analysis was used to assess the protein level. As shown in Fig. 4a and c, SNL induced the overexpression of PKCε and TRPV1(all $P<0.05$). Fortunately, in line with pain relief, consecutive administration with PF alleviated the upregulation of PKCε and TRPV1(all $P<0.05$). In addition, the qPCR assay (Fig. 3d and e) showed the same general trend of expression at the mRNA level of PKCε and TRPV1 with the protein level (all $P<0.05$). Of note, no significance difference was

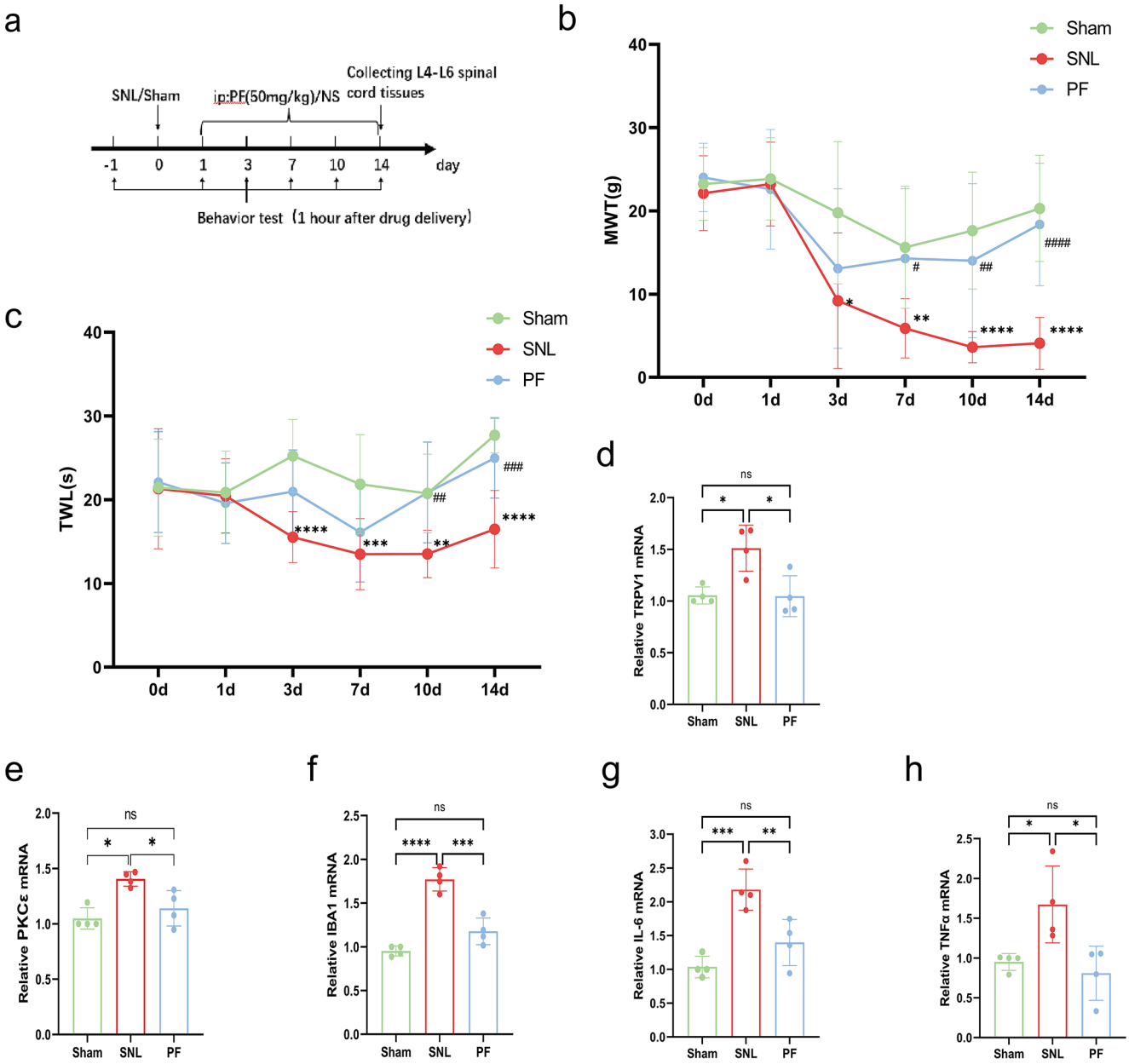

Fig. 3 Animal experimental behavioral assessment and qPCR results. (**a**) Schematic diagram of animal experimental procedure manipulation. (**b**) Changes in MWT between Sham, SNL, and SNL-PF treatment groups (PF), data are expressed as mean±SD ($n=12$). Statistical significance was determined using a two-way ANOVA with Tukey's post-hoc test, compared with the sham group $^{*}P<0.05$, $^{**}P<0.01$, $^{***}P<0.001$, $^{****}P<0.0001$; compared with the SNL group, $^{\#}P<0.05$, $^{\#\#}P<0.01$, $^{\#\#\#}P<0.001$, $^{\#\ \#\#\#}P<0.0001$. (**c**) Changes in TWL in the Sham, SNL, and SNL-PF treatment groups (PF), and the data were expressed as mean±SD ($n=12$). Statistical significance was determined using a two-way ANOVA with Tukey's post-hoc test, compared with the sham group, $^{*}P<0.05$, $^{**}P<0.01$; compared with the SNL group, $^{\#}P<0.05$, $^{\#\#}P<0.01$. (**d-h**) mRNA expression levels of TRPV1(**d**), PKCε(**e**), IBA1(**f**), IL-6(g), and TNF-α(**h**) mRNA, and the data were expressed as mean±SD ($n=6$). In figures (**e**) and (**h**), the Kruskal-Wallis non-parametric test was used to compare the Sham group with the other two groups, while a one-way ANOVA followed by Tukey's post-hoc test was employed for the remaining comparisons, $^{*}P<0.05$, $^{**}P<0.01$, $^{***}P<0.001$, $^{****}P<0.0001$

observed between the Sham group and the PF group. Additionally, molecular docking was performed to verify the regulatory effect of PF on PKCε and TRPV1. As shown in Table 3; Fig. 5p and q, PF can bind tightly to the PKCε protein (binding energies = -8 kcal/mol) at the same site where PKC inhibitor Sotrastaurin binds to PKCε (binding energies = -8.9 kcal/mol), suggesting that PF functions as a PKCε inhibitor. At the same time, Fig. 5r and s demonstrate that PF can act as a TRPV1 antagonist (The binding energies

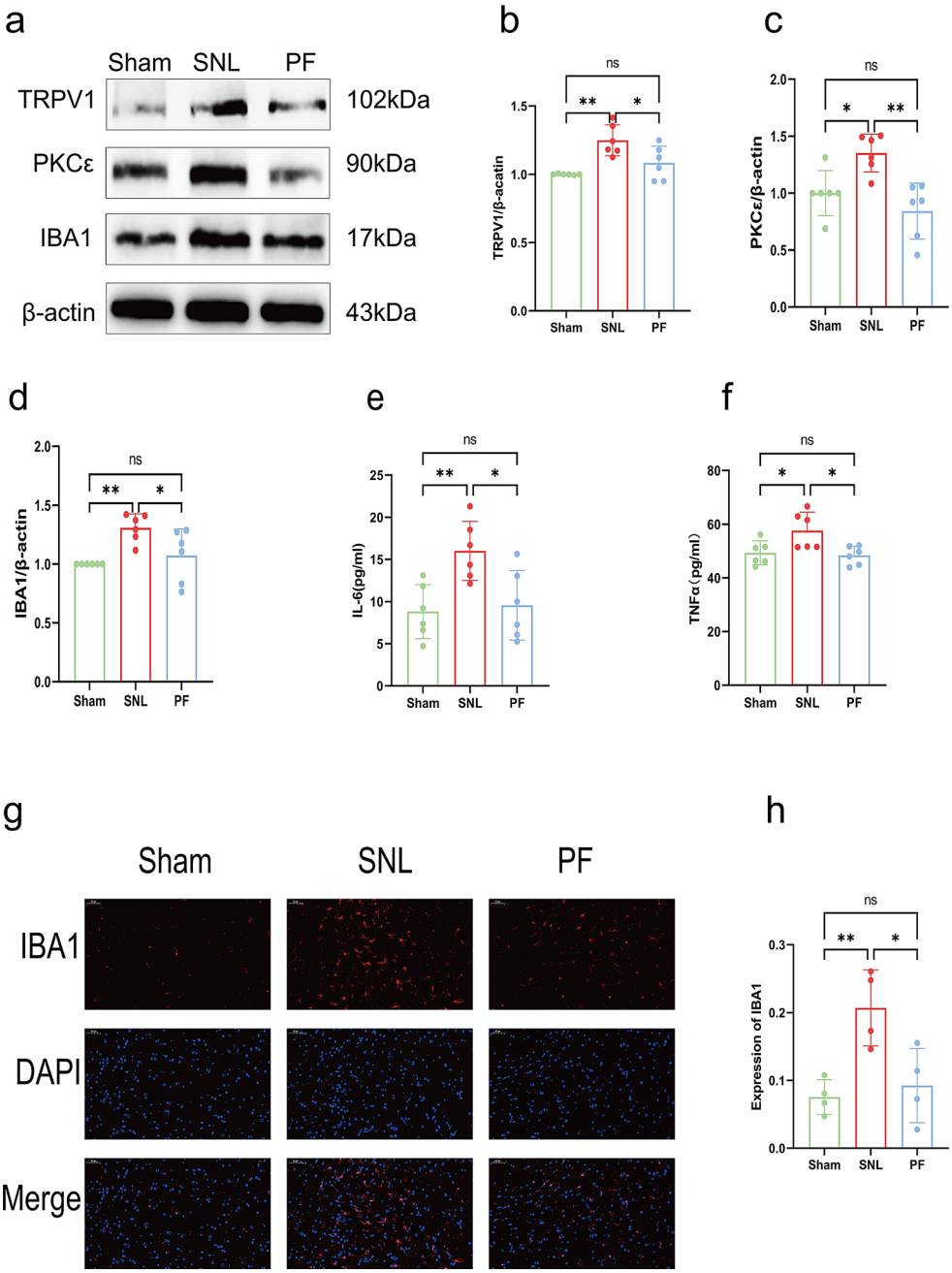

Fig. 4 Western blotting, ELISA and Immunofluorescence results. Statistical significance between groups was determined using a one-way ANOVA followed by Tukey's post-hoc test, $^{*}P<0.05$, $^{**}P<0.01$. (**a**) Western blotting to detect the expression levels of TRPV1, PKCε, and IBA1. (**b**-**d**) Relative quantitative analysis of TRPV1, PKCε, and IBA1 ($n=6$). (**e**, **f**) ELISA for IL-6, TNF-α expression level ($n=6$). (**g**) Immunofluorescence staining of microglia in the dorsal horn of the spinal cord (Scale bar = 50 μm). (**h**) Relative quantitative analysis of microglia in the dorsal horn of the spinal cord ($n=4$)

of PF and SB-366791withTRPV1 protein are respectively −8.1 kcal/mol and −8.2 kcal/mol).

PF Reduced the Production of IL-6, TNF-α Inflammatory Factors

According to the results of our network pharmacology analysis IL-6 and TNF-α were predicted to be the key targets of PF for the therapy of NP. The ELISA and qPCR analysis were used to investigate further the role of PF in reducing the expression of inflammatory factors IL-6 and TNF-α. As shown in Fig. 4e and f, PF administration significantly suppressed the SNL-induced upregulation of IL-6 and TNF-α in the spinal cord (all $P<0.05$). The qPCR results showed the same general trend (Fig. 3g and h). As well as, no significant difference between the PF groups and the Sham group. Furthermore, the molecular docking results indicate that PF exhibits a strong affinity for the core targets IL-6 and TNF-α (Fig. 5a and b). Their lowest binding energies are respectively −8 kcal/mol and −9 kcal/mol.

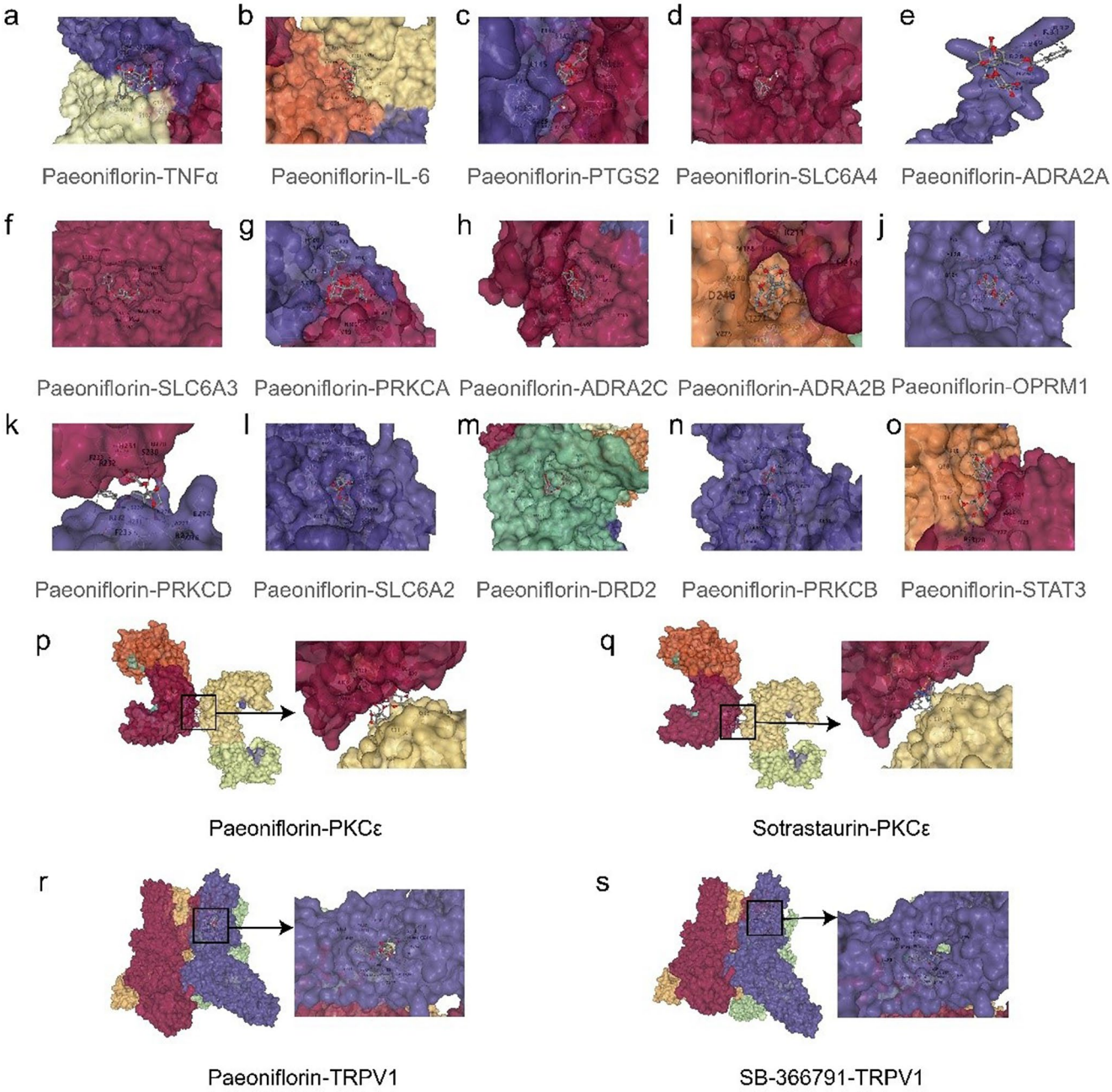

Fig. 5 Results of molecular docking. (**a**-**o**) The molecular docking detailed diagrams of paeoniflorin and TNF-α(**a**), IL 6(**b**),PTGS2(**c**), SLC6A4(**d**),ADRA2A(**e**),SLC6A3(**f**),PRKCA(**g**),ADRA2C(**h**),ADRA2B(**i**),OPRM1(**j**),PRKCD(**k**),SLC6A2(**l**),DRD2(**m**),PRKCB(**n**),STAT(**o**). (**p**) paeoniflorin can bind tightly to the PKCε protein, and the lowest binding energies = -8 kcal/mol. On the right is a detailed diagram of the ligand-protein docking. (**q**) PKC inhibitor Sotrastaurin binds to PKCε, and the lowest binding energy is -8.9 kcal/mol. On the right is a detailed diagram of the ligand-protein docking. (**r**) paeoniflorin is docked with TRPV1 protein, and the lowest binding energy is -8.1 kcal/mol. On the right is a detailed diagram of the ligand-protein docking. (**s**) TRPV1 antagonist SB-366791 is docked with TRPV1, and the binding energy is -8.2 kcal/mol). On the right is a detailed diagram of the ligand-protein docking

PF Ameliorated NP by Inhibiting Microglia Activation in the Dorsal Horn of the Spinal Cord

Given the crucial role of microglial activation in NP, we investigated the effect of PF on regulating microglial activation in the spinal cord to elucidate the molecular mechanisms underlying PF's alleviation of NP. As previously described, microglial activation was assessed by examining changes in the number and morphology of IBA1-positive cells in the dorsal horn of the spinal cord [21]. Firstly, we evaluated the expression of the microglial marker IBA1 at both the protein and mRNA levels in the spinal cord, Western blotting

and qPCR results revealed that SNL significantly upregulated IBA1 expression, an effect that was reversed by PF administration (all $P<0.05$) (Figs. 3f and 4a and d). Secondly, as illustrated in Fig. 4g and h, SNL induced substantial morphological changes and increased accumulation of IBA1-stained microglia in the dorsal horn ($P<0.01$). In contrast, these SNL -induced alterations in microglial morphology and accumulation were markedly attenuated by PF treatment ($P<0.05$).

Discussion

The development of society and the increase in life pressure have led to a rising incidence of NP, which significantly impacts the quality of life and imposes a substantial social and economic burden. PF, a natural compound, exhibits significant anti-inflammatory and immunomodulatory effects, as well as, has the characteristics of being non-toxic and harmless [6]. Through network pharmacology studies, we found that PF can effectively target multiple mechanisms associated with NP. These mechanisms include the regulation of specific molecular functions such as adrenergic receptors, PKCs, and 5-HT receptors, as well as the involvement of the Ca^{2+} signaling pathway, the regulation of TRP channels by inflammatory mediators, and GPCRs signaling pathways.

GPCRs are membrane proteins with binding sites for guanylate binding proteins, which can sense various chemical signals from the extracellular matrix and transmit these signals into the cell [22]. Opioid receptors, cannabinoid receptors, α2-adrenergic receptors, and other GPCRs are involved in the development and maintenance of NP and have become important targets for various analgesic drugs [23]. As revealed by our network pharmacology analysis, OPRM1, a member of the opioid G protein-coupled receptor family, has been shown to exhibit significant neuroplasticity in NP. Studies indicate that peripheral nerve injury, such as sciatic nerve damage, significantly downregulates the expression of the OPRM1 gene and reduces the responsiveness of OPRM1-expressing neurons to selective agonists [24]. The molecular docking results demonstrate a stable binding interaction between PF and the OPRM1 protein, with a binding energy of -9 kcal/mol. The docking analysis reveals that PF can form multiple hydrogen bonds and hydrophobic interactions with key amino acid residues in the active site of the OPRM1 protein. Although direct experimental evidence is currently lacking to confirm that PF specifically targets the OPRM1 gene or its encoded μ-opioid receptor, existing studies suggest that PF may influence opioid receptor activity by modulating the overall function of the nervous system [25]. Particularly in the treatment of NP, PF may indirectly regulate opioid receptor signaling pathways through a multi-target mechanism, thereby exerting its analgesic effects. Adrenergic receptors, as G-protein-coupled receptors, also play a crucial role in regulating pain sensitivity. In the context of NP, norepinephrine mediates an anti-nociceptive effect primarily through the activation of α2-adrenergic receptors located in the dorsal horn of the spinal cord. α2-adrenergic receptors, coupled with inhibitory G proteins, inhibit the release of excitatory neurotransmitters from primary afferent fibers by inhibiting presynaptic voltage-gated Ca^{2+} channels in the dorsal horn of the spinal cord, reducing the occurrence of pain [26]. Ca^{2+} channels are essential for the initiation, conduction, and repetitive firing of action potentials, as well as neurotransmitter release following nerve damage. In particular, CaV 2.2 and CaV 3.1 have been identified as potential targets for treating NP [27, 28]. Our network pharmacology analysis also revealed that ADRA2A, ADRA2B, and ADRA2C play an important role in alleviating NP by PF. Furthermore, the molecular docking analysis results indicate they can all form stable complexes with PF. Previous studies have shown that PF increases the release of norepinephrine and activates α2-adrenergic receptors to regulate injury-mediated spinal cord transmission in diabetic neuropathy [29]. It is noteworthy that although these results suggest potential interactions between PF and adrenergic receptors, the specific mechanisms of action and biological effects still require systematic experimental validation.

5-HT, a neurotransmitter extensively distributed across the cerebral cortex and synapses, is integral to regulating various physiological processes, including pain, sleep, and mood [30]. The role of 5-HT in pain regulation is notably complex and multifaceted, influenced by receptor subtypes, sites of action, and downstream neural circuits. 5-HT-mediated brainstem activity is pivotal in the development of central pain sensitization [31]. However, when 5-HT projections from the periaqueductal gray activate inhibitory interneurons in the dorsal horn of the spinal cord, they suppress dorsal horn neuron activity and inhibit pain signal transmission [32]. In the spinal cord, 5-HT receptors are predominantly G protein-coupled, except for the 5-HT3 receptors, which are a ligand-gated ion channel. These receptors are located on primary afferent fibers, thalamic projection neurons, local interneurons, and descending projections, including 5-HTergic neurons [33]. Their effects on pain perception vary by subtype. For instance, 5-HT1A receptor activation in the spinal cord generally yields antinociceptive effects in NP, whereas 5-HT3 receptors can both promote and inhibit pain, potentially due to differences in binding affinity [30]. Our network pharmacology analysis indicates that 5-HT2 receptors—specifically 5-HTR2A, 5-HTR2B, and 5-HTR2C—are primarily involved in the mechanism by which PF alleviates NP. Notably, the 5-HTR2A receptor has been shown to promote local NP but inhibit hyperalgesia at the spinal level. The role of the 5-HTR2B receptor in NP appears to be contingent on

neuroimmune mechanisms, while the 5-HTR2C receptor primarily exerts antihyperalgesic effects in the spinal cord [30]. While direct evidence of PF interacting with 5-HT2 receptors is absent, its various pharmacological effects, including neuroprotective, anti-inflammatory, and analgesic properties, imply it may indirectly modulate these receptors. The molecular docking study further reveals that PF can directly bind to the active site of the 5-HT transporter (SLC6A4) with a binding energy of -10.1 kcal/mol. This finding suggests that PF may influence the activity of the serotonin system by modulating the function of the serotonin transporter, thereby exerting its neuroprotective effects. Furthermore, our study suggests that 5-HT2 receptors are involved in regulating TRP channels. Evidence from Caenorhabditis elegans indicates that the release of 5-HT depends on TRPV1 channel activation in 5-HTergic neurons, with TRP channels modulating monoamine release in these neuronal subpopulations [34]. In NP models, both 5-HT1A and TRPV1 receptors influence the firing activity of 5-HT neurons in the dorsal raphe nucleus, although their regulatory roles in the spinal cord require further elucidation and in-depth investigation [35].

TRPV1, a nonselective cationic channel, functions as a Ca^{2+}permeable channel and regulates Ca^{2+} influx [36]. This ion channel is activated by capsaicin and heat, and is expressed by peripheral injury receptors, implicating it in various inflammatory and NP disorder [37]. A substantial body of research has highlighted the critical role of TRPV1 in NP. In diabetic mouse models, the TRPV1 ion channel is highly expressed in nociceptive dorsal root ganglion (DRG) neurons, where its activation induces rapid current generation in both heterologous cells and nociceptive DRG neurons [38]. Similarly, in rat models of chronic sciatic nerve compression injury, the expression of TRPV1 is progressively upregulated in the dorsal horn of the spinal cord. Additionally, intrathecal administration of TRPV1 antagonists has been shown to effectively inhibit hyperalgesia, underscoring the therapeutic potential of targeting this ion channel [39]. Clinical trials conducted by Arendt-Nielsen et al. further support these findings, demonstrating that TRPV1 antagonists significantly increase the threshold for capsaicin-induced heat and mechanical pain in healthy volunteers [40]. Yuanyuan Li et al. showed that paclitaxel-induced peripheral NP could be mitigated by inhibiting TRPV1 upregulation through electroacupuncture [41]. In addition, PF has been shown to inhibit TRPV1 activation and reduce the inflammatory pain associated with it [42]. Complementing these insights, our animal experiments and molecular docking studies confirmed that PF can directly bind to TRPV1 protein, functioning as a TRPV1 antagonist. Additionally, network pharmacological analyses suggest that the analgesic mechanism of PF may involve the modulation of various subtypes of 5-HT receptors. However, the precise role of specific 5-HT receptor subtypes, particularly 5-HT2 receptor, in pain relief requires further investigation to elucidate the underlying mechanisms.

The previous study has also underscored the critical role of PKC activation, particularly PKCε, in the sensitization of TRPV1 activation [43]. PKC, a serine/threonine kinase, serves as an effector in the GPCR system and is recognized as a pivotal enzyme in signal transduction mechanisms across various biological processes [44]. Our network pharmacology analyses have identified a strong correlation between PKCs and GPCRs in the molecular mechanisms underlying the action of PF in alleviating NP. PKCs are categorized into three subfamilies based on their structural and activation characteristics. The first subfamily, conventional PKCs, includes PKCα, βI, βII, and γ, which require both diacylglycerol (DAG) and Ca2 + for activation. The second subfamily, novel PKCs, comprises PKCδ, ε, η, and θ, which require only DAG for activation. Members of these two subfamilies exhibit comparable affinities for membrane binding. The third subfamily, atypical PKCs, includes PKCζ, λ, and ι, which are neither activated by DAG nor Ca2+ [45–47]. Network pharmacological analyses have further revealed that PKC isoforms (such as PKCα, PKCβ, PKCγ, PKCη, PKCε) are potential targets for PF in alleviating NP. In addition, molecular docking analysis indicates that PF exhibits favorable binding properties with multiple potential targets, including PKCα, PKCβ, PKCδ, and PKCε. In chronic diabetic neuropathy, the upregulation of PKCε is associated with thermal and mechanical hyperalgesia in the development of pain processes [48]. In the SNI model, upregulation of PKCε results in peripheral sensitization and increased pain sensitivity in rats [49]. This pain sensitization is further exacerbated by the interaction between PKCε and TRPV1 [50]. In addition, Chen et al. ‘s experimental study showed that PF combined with liquiritigenin may inhibit PKC signal transmission by coordinating calcium signal and lipid metabolism, thereby alleviating NP [51]. It is suggested that PF may play a role in PKC signal regulation. However, they only showed the simultaneous role of the two compounds, but did not analyze the role of PF in calcium signaling and PKC signaling alone. We used molecular docking to compare the binding degree between PF and PKCε protein with the PKC inhibitor Sotrastarin and PKCε protein. The experimental results showed that PF and Sotrastarin can highly bind with PKCε at the same site of PKCε. It is suggested that PF may act as an inhibitor of PKCε to relieve NP.

Based on PPI network analysis, we investigated the mRNA expression of inflammatory factors IL-6 and TNF-α in the spinal cord using qPCR, and their protein levels using ELISA. Both the gene and protein levels of IL-6 and TNF-α were significantly elevated in the SNL group compared to the Sham group. However, PF treatment significantly reduced the expression levels of these inflammatory

cytokines. These cytokines, released by activated microglia, play a crucial role in the inflammatory response following nerve injury through intracellular mediators such as PKC. They also contribute to the sensitization of the central nervous system, potentially leading to abnormal pain [2]. The enhanced peripheral and central expression of these pro-inflammatory cytokines in response to nerve injury increases excitation and decreases inhibition of interneurons, thereby causing pain symptoms [52]. To further elucidate the molecular mechanism by which PF alleviates NP, we examined the effect of PF on the activation state of microglia. Immunofluorescence and western blotting results demonstrated that SNL induced microglia activation in the dorsal horn of the spinal cord and increased microglia protein expression. PF intervention was found to mitigate the activation of microglia induced by nerve injury.

Under normal conditions, microglia account for less than 20% of spinal cord glial cells [53]. However, following nerve injury, mediators such as neuromodulin-1, matrix metalloproteinase (MMP)-2, MMP-9, and chemokine ligand 2 are released, leading to the rapid proliferation and activation of microglia in the dorsal root ganglia and spinal cord. This abnormal activation of spinal cord microglia is implicated in the formation, development, maintenance, and enhancement of NP [54]. Our Western blotting and Immunofluorescence studies corroborate these findings, demonstrating significant microglial activation post-injury. Upon activation, microglia stimulate the complement component of the immune system and release cytokines, chemokines, and cytotoxic substances, creating a pro-inflammatory environment that originates at synaptic sites in the brainstem and the site of neurological injury, subsequently spreading to additional locations [2, 52]. Our Immunofluorescence results further indicate that PF can significantly inhibit microglial activation in the dorsal horn of the spinal cord. This further suggests that the anti-inflammatory effect of PF is related to the inhibition of microglia activation. Recent experimental literature indicates that PF can suppress microglial activation, which may subsequently mitigate the release of pro-inflammatory mediators known to exacerbate neuronal damage [11]. Moreover, studies have shown that PF significantly reduces the expression of pro-inflammatory cytokines, including TNF-α, IL-1β, and IL-6, in neuroinflammation models [13]. These findings align with our observations and suggest that the anti-inflammatory effects of PF are likely a critical component of its neuroprotective mechanisms.

Additionally, TRPV1 plays an important role in microglial activation in vivo. TRPV1 -mediated activation of the NOD-, LRR-, and pyrin domain-containing protein 3 (NLRP3) inflammasome via the Ca^{2+} pathway in microglia leads to neuroinflammation, while TRPV1 ablation effectively inhibits this process [55]. Other studies have also reported that controlled activation of TRPV1 channels on microglia can enhance autophagy, thereby potentially improving neurodegenerative diseases [56]. Regrettably, while we have investigated the status of TRPV1 and microglial activation as well as the effect of PF on these processes, we have not explored the interaction between TRPV1 and microglial activation in greater depth.

This study has several limitations that should be acknowledged. Firstly, the network pharmacology analysis identified numerous key signaling pathways and related targets, including adrenergic receptors, the GPCR signaling pathway, and Ca^{2+} signaling pathways. These findings warrant further experimental validation to confirm their roles and implications. Additionally, the selection of a single dose for PF was based on existing literature and preliminary experimental results. This approach limited our ability to fully ascertain the optimal dose for NP and to achieve the best possible therapeutic effect. Future studies should consider exploring a range of doses to better determine the most effective treatment regimen. Finally, the study's breadth, depth, and accuracy were limited by using only male rats and excluding females.

Conclusions

Combined with network pharmacology analysis, animal studies, and molecular docking, we have concluded that PF can treat NP by modulating multiple signaling pathways and target proteins involved in pain perception and inflammation. The experimental results further confirmed that PF can significantly alleviate the pain behavior in rats with SNL-induced NP. Notably, PF was found to significantly inhibit the activity of PKC and TRPV1 in the spinal cord, and can act as an inhibitor of PKCε and an antagonist of TRPV1. Additionally, PF significantly suppressed microglial activation and neuroinflammatory responses. These findings provide a novel reference for NP treatment and suggest the potential analgesic role of PF in the clinical treatment of NP.

Author Contributions All authors contributed to the study's conception and design. F.X.,Q.L.and L.Z. wrote the first draft of the manuscript. F.X.,S.C., Q. Y., and Y. Z.performed the animal experiments.F.X., Z. L., H. Z. carried out data analyses. All authors commented on previous versions of the manuscript. All authors read and approved the final manuscript.

Funding The authors declare that no funds, grants, or other support were received during the preparation of this manuscript.

Data Availability Data is provided within the manuscript.

Declarations

Competing Interests The authors declare no competing interests.

References

1. Vieira WF, Coelho DRA, Litwiler ST et al (2024) Neuropathic pain, mood, and stress-related disorders: A literature review of comorbidity and co-pathogenesis. Neurosci Biobehavioral Reviews 161:105673. https://doi.org/10.1016/j.neubiorev.2024.105673
2. Cohen SP, Mao J (2014) Neuropathic pain: mechanisms and their clinical implications. BMJ 348:f7656. https://doi.org/10.1136/bmj.f7656
3. Gilron I, Baron R, Jensen T (2015) Neuropathic pain: principles of diagnosis and treatment. Mayo Clin Proc 90(4):532–545. https://doi.org/10.1016/j.mayocp.2015.01.018
4. Finnerup NB, Kuner R, Jensen TS (2021) Neuropathic pain: from mechanisms to treatment. Physiol Rev 101(1):259–301. https://doi.org/10.1152/physrev.00045.2019
5. China Pharmaceutical Science and Technology Press (2020) National Pharmacopoeia Commission. One Part of the Chinese Pharmacopoeia. Beijing
6. Zhang LL, Wei W (2020) Anti-inflammatory and immunoregulatory effects of paeoniflorin and total glucosides of paeony. Pharmacology & Therapeutics 207. DOI: ARTN 10745210.1016/j.pharmthera.2019.107452
7. Jiang H, Li J, Wang L et al (2020) Total glucosides of Paeony: A review of its phytochemistry, role in autoimmune diseases, and mechanisms of action. J Ethnopharmacol 258:112913. https://doi.org/10.1016/j.jep.2020.112913
8. Fan YX, Qian C, Liu B et al (2018) Induction of suppressor of cytokine signaling 3 via HSF-1-HSP70-TLR4 axis attenuates neuroinflammation and ameliorates postoperative pain. Brain Behav Immun 68:111–122. https://doi.org/10.1016/j.bbi.2017.10.006
9. Andoh T, Goto M (2023) Repeated topical Paeoniflorin attenuates postoperative pain and accelerates cutaneous fibroblast proliferation in mice. J Pharmacol Sci 151(2):84–87. https://doi.org/10.1016/j.jphs.2022.12.004
10. Ding X, Sun Y, Wang Q et al (2016) Pharmacokinetics and pharmacodynamics of glycyrrhetinic acid with Paeoniflorin after transdermal administration in dysmenorrhea model mice. Phytomedicine 23(8):864–871. https://doi.org/10.1016/j.phymed.2016.05.005
11. Zhou D, Zhang S, Hu L et al (2019) Inhibition of apoptosis signal-regulating kinase by Paeoniflorin attenuates neuroinflammation and ameliorates neuropathic pain. J Neuroinflammation 16(1):83. https://doi.org/10.1186/s12974-019-1476-6
12. Andoh T, Kobayashi N, Uta D, Kuraishi Y(2016)Prophylactic topical Paeoniflorin prevents mechanical allodynia caused by Paclitaxel in mice through adenosine A1 receptors. Phytomedicine 25:1–7. https://doi.org/10.1016/j.phymed.2016.12.010
13. Guo Q, Li W, Wang C et al (2020) Biomolecular network-based synergistic drug combination discovery: a combination of Paeoniflorin and liquiritin alleviates neuropathic pain by inhibiting neuroinflammation via suppressing the chemokine signaling pathway. Signal Transduct Target Ther 5(1):73. https://doi.org/10.1038/s41392-020-0160-8
14. Zhao L, Zhang H, Li N et al (2023) Network Pharmacology, a promising approach to reveal the Pharmacology mechanism of Chinese medicine formula. J Ethnopharmacol 309:116306. https://doi.org/10.1016/j.jep.2023.116306
15. Duan ZL, Wang YJ, Lu ZH et al (2023) Wumei Wan attenuates angiogenesis and inflammation by modulating RAGE signaling pathway in IBD: network Pharmacology analysis and experimental evidence. Phytomedicine 111:154658. https://doi.org/10.1016/j.phymed.2023.154658
16. Ho Kim S, Mo Chung J (1992) An experimental model for peripheral neuropathy produced by segmental spinal nerve ligation in the rat. Pain 50(3):355–363. https://doi.org/10.1016/0304-3959(92)90041-9
17. Liu P, Cheng J, Ma S, Zhou J (2020) Paeoniflorin attenuates chronic constriction injury-induced neuropathic pain by suppressing spinal NLRP3 inflammasome activation. Inflammopharmacology 28(6):1495–1508. https://doi.org/10.1007/s10787-020-00737-z
18. Chaplan SR, Bach FW, Pogrel JW, Chung JM, Yaksh TL (1994) Quantitative assessment of tactile allodynia in the rat paw. J Neurosci Methods 53(1):55–63. https://doi.org/10.1016/0165-0270(94)90144-9
19. Shuyuan L, Haoyu C (2023) Mechanism of nardostachyos Radix et Rhizoma-Salidroside in the treatment of premature ventricular beats based on network Pharmacology and molecular Docking. Sci Rep 13(1):20741. https://doi.org/10.1038/s41598-023-48277-0
20. Chen S, Li B, Chen L, Jiang H (2023) Uncovering the mechanism of Resveratrol in the treatment of diabetic kidney disease based on network pharmacology, molecular docking, and experimental validation. J Transl Med 21(1):380. https://doi.org/10.1186/s12967-023-04233-0
21. Zhang LQ, Gao SJ, Sun J et al (2022) DKK3 ameliorates neuropathic pain via inhibiting ASK-1/JNK/p-38-mediated microglia polarization and neuroinflammation. J Neuroinflammation 19(1):129. https://doi.org/10.1186/s12974-022-02495-x
22. Congreve M, de Graaf C, Swain NA, Tate CG (2020) Impact of GPCR structures on drug discovery. Cell 181(1):81–91. https://doi.org/10.1016/j.cell.2020.03.003
23. Limerick G, Uniyal A, Ford N et al (2024) Peripherally restricted cannabinoid and mu-opioid receptor agonists synergistically attenuate neuropathic mechanical hypersensitivity in mice. Pain 165(11):2563–2577. https://doi.org/10.1097/j.pain.0000000000003278
24. Qi Y, Nelson TS, Prasoon P et al (2023) Contribution of M opioid Receptor-expressing dorsal Horn interneurons to neuropathic Pain-like behavior in mice. Anesthesiology 139(6):840–857. https://doi.org/10.1097/ALN.0000000000004735
25. Zhang XJ, Li Z, Leung WM et al (2008) The analgesic effect of Paeoniflorin on neonatal maternal separation-induced visceral hyperalgesia in rats. J Pain 9(6):497–505. https://doi.org/10.1016/j.jpain.2007.12.009
26. Huang Y, Chen H, Chen SR, Pan HL (2023) Duloxetine and amitriptyline reduce neuropathic pain by inhibiting primary sensory

input to spinal dorsal Horn neurons via α1- and α2-Adrenergic receptors. ACS Chem Neurosci 14(7):1261–1277. https://doi.org/10.1021/acschemneuro.2c00780
27. Bear B, Asgian J, Termin A, Zimmermann N (2009) Small molecules targeting sodium and calcium channels for neuropathic pain. Curr Opin Drug Discov Devel 12(4):543–561. https://www.ncbi.nlm.nih.gov/pubmed/19562650
28. Zamponi GW, Striessnig J, Koschak A, Dolphin AC (2015) The physiology, pathology, and Pharmacology of Voltage-Gated calcium channels and their future therapeutic potential. Pharmacol Rev 67(4):821–870. https://doi.org/10.1124/pr.114.009654
29. Lee KK, Omiya Y, Yuzurihara M, Kase Y, Kobayashi H (2011) Antinociceptive effect of Paeoniflorin via spinal α_2-adrenoceptor activation in diabetic mice. Eur J Pain 15(10):1035–1039. https://doi.org/10.1016/j.ejpain.2011.04.011
30. Liu QQ, Yao XX, Gao SH et al (2020) Role of 5-HT receptors in neuropathic pain: potential therapeutic implications. Pharmacol Res 159:104949. https://doi.org/10.1016/j.phrs.2020.104949
31. Suzuki R, Rygh LJ, Dickenson AH (2004) Bad news from the brain: descending 5-HT pathways that control spinal pain processing. Trends Pharmacol Sci 25(12):613–617. https://doi.org/10.1016/j.tips.2004.10.002
32. Sommer C (2004) Serotonin in pain and analgesia: actions in the periphery. Mol Neurobiol 30(2):117–125. https://doi.org/10.1385/MN:30:2
33. Mokhtar N, Doly S, Courteix C (2023) Diabetic neuropathic pain and serotonin: what is new in the last 15 years?? Biomedicines 11(7):1924. https://doi.org/10.3390/biomedicines11071924
34. Oakes M, Law WJ, Komuniecki R (2019) Cannabinoids stimulate the TRP Channel-Dependent release of both serotonin and dopamine to modulate behavior in C. elegans. J Neurosci 39(21):4142–4152. https://doi.org/10.1523/JNEUROSCI.2371-18.2019
35. De Gregorio D, McLaughlin RJ, Posa L et al (2019) Cannabidiol modulates serotonergic transmission and reverses both allodynia and anxiety-like behavior in a model of neuropathic pain. Pain 160(1):136–150. https://doi.org/10.1097/j.pain.0000000000001386
36. Oh SJ, Lim JY, Son MK et al (2023) TRPV1 Inhibition overcomes cisplatin resistance by blocking autophagy-mediated hyperactivation of EGFR signaling pathway. Nat Commun 14(1):2691. https://doi.org/10.1038/s41467-023-38318-7
37. Yue WWS, Yuan L, Braz JM, Basbaum AI, Julius D (2022) TRPV1 drugs alter core body temperature via central projections of primary afferent sensory neurons. Elife 11. https://doi.org/10.7554/eLife.80139
38. Xie YK, Luo H, Zhang SX et al (2022) GPR177 in A-fiber sensory neurons drives diabetic neuropathic pain via WNT-mediated TRPV1 activation. Sci Transl Med 14(639):eabh2557. https://doi.org/10.1126/scitranslmed.abh2557
39. Kanai Y, Nakazato E, Fujiuchi A, Hara T, Imai A (2005) Involvement of an increased spinal TRPV1 sensitization through its up-regulation in mechanical allodynia of CCI rats. Neuropharmacology 49(7):977–984. https://doi.org/10.1016/j.neuropharm.2005.05.003Epub 2005 Jul 5
40. Arendt-Nielsen L, Harris S, Whiteside GT et al (2016) A randomized, double-blind, positive-controlled, 3-way cross-over human experimental pain study of a TRPV1 antagonist (V116517) in healthy volunteers and comparison with preclinical profile. Pain 157(9):2057–2067. https://doi.org/10.1097/j.pain.0000000000000610
41. Li Y, Yin C, Li X et al (2019)Electroacupuncture alleviates Paclitaxel-Induced peripheral neuropathic pain in rats via suppressing TLR4 signaling and TRPV1 upregulation in sensory neurons. Int J Mol Sci 20(23). https://doi.org/10.3390/ijms20235917
42. Ruan Y, Ling J, Ye F et al (2021) Paeoniflorin alleviates CFA-induced inflammatory pain by inhibiting TRPV1 and succinate/SUCNR1-HIF-1alpha/NLPR3 pathway. Int Immunopharmacol 101(Pt B) 108364. https://doi.org/10.1016/j.intimp.2021.108364
43. Zhu W, Xu P, Cuascut FX, Hall AK, Oxford GS (2007) Activin acutely sensitizes dorsal root ganglion neurons and induces hyperalgesia via PKC-mediated potentiation of transient receptor potential vanilloid I. J Neurosci 27(50):13770–13780. https://doi.org/10.1523/JNEUROSCI.3822-07.2007
44. Serlachius E, Svennilson J, Schalling M, Aperia A (1997) Protein kinase C in the developing kidney: isoform expression and effects of ceramide and PKC inhibitors. Kidney Int 52(4):901–910. https://doi.org/10.1038/ki.1997.411
45. Gorin MA, Pan Q (2009) Protein kinase C epsilon: an oncogene and emerging tumor biomarker. Mol Cancer 8:9. https://doi.org/10.1186/1476-4598-8-9
46. Kawano T, Inokuchi J, Eto M, Murata M, Kang JH (2021) Activators and inhibitors of protein kinase C (PKC): their applications in clinical trials. Pharmaceutics 13(11). https://doi.org/10.3390/pharmaceutics13111748
47. Isakov N (2018) Protein kinase C (PKC) isoforms in cancer, tumor promotion and tumor suppression. Semin Cancer Biol 48:36–52. https://doi.org/10.1016/j.semcancer.2017.04.012
48. Kan YY, Chang YS, Liao WC, Chao TN, Hsieh YL (2024) Roles of neuronal protein kinase Cepsilon on Endoplasmic reticulum stress and autophagic formation in diabetic neuropathy. Mol Neurobiol 61(5):2481–2495. https://doi.org/10.1007/s12035-023-03716-x
49. Xu J, Wu S, Wang J et al (2021) Oxidative stress induced by NOX2 contributes to neuropathic pain via plasma membrane translocation of PKCepsilon in rat dorsal root ganglion neurons. J Neuroinflammation 18(1):106. https://doi.org/10.1186/s12974-021-02155-6
50. Zhao X, Xia B, Cheng J, Zhu MX, Li Y (2020) PKCepsilon sumoylation is required for mediating the nociceptive signaling of inflammatory pain. Cell Rep 33(1):108191. https://doi.org/10.1016/j.celrep.2020.108191
51. Chen YY, Feng LM, Xu DQ et al (2022) Combination of Paeoniflorin and liquiritin alleviates neuropathic pain by lipid metabolism and calcium signaling coordination. Front Pharmacol 13:944386. https://doi.org/10.3389/fphar.2022.944386
52. Zhao H, Alam A, Chen Q et al (2017) The role of microglia in the pathobiology of neuropathic pain development: what do we know? Br J Anaesth 118(4):504–516. https://doi.org/10.1093/bja/aex006
53. Fu R, Shen Q, Xu P, Luo JJ, Tang Y (2014) Phagocytosis of microglia in the central nervous system diseases. Mol Neurobiol 49(3):1422–1434. https://doi.org/10.1007/s12035-013-8620-6
54. Liu Q, Li R, Yang W, Cui R, Li B (2021) Role of neuroglia in neuropathic pain and depression. Pharmacol Res 174:105957. https://doi.org/10.1016/j.phrs.2021.105957
55. Zhang Y, Hou B, Liang P et al (2021) TRPV1 channel mediates NLRP3 inflammasome-dependent neuroinflammation in microglia. Cell Death Dis 12(12):1159. https://doi.org/10.1038/s41419-021-04450-9
56. Yuan J, Liu H, Zhang H, Wang T, Zheng Q, Li Z (2022) Controlled activation of TRPV1 channels on microglia to boost their autophagy for clearance of Alpha-Synuclein and enhance therapy of Parkinson's disease. Adv Mater 34(11):e2108435. https://doi.org/10.1002/adma.202108435